ELECTRONICS AND ELECTRICAL ENGINEERING
ISSN 1392 – 1215 *2008. No. 5(85)*
ELEKTRONIKA IR ELEKTROTECHNIKA

ELECTRICAL ENGINEERING
T190
ELEKTROS INŽINERIJA

Approach to Efficiency of the Low Frequency Inductive Heating of Ferromagnetics

B. Miedzinski, Z. Okraszewski
Wroclaw University of Technology, Institute of Electric Power Engineering,
Wybrzeze Wyspianskiego 27,50-370, Wroclaw, Poland, phone +48 71 3203693, e-mail: bogdan.miedzinski@pwr.wroc.pl
X. Wang, Lj. Xu
Beijing University of Posts and Telecommunications, Research Laboratory of Electric Contacts,
Xi Tu Cheng Road 10, Beijing, China, phone +86 10 62283173, e-mail: wangxin820117@gmail.com

Introduction

It was found that a low frequency inductive heating can be used successfully for various specified applications among others for heating procedure of railway rails under track laying [1]. However to perform it properly one has to consider carefully the phenomena related to heating and develop the rails heating strategy as well. Therefore, in this paper the calculations results of the heating efficiency of the railway rail depending on frequency, supplying MMF value and location of the heater are presented and discussed.

The simulations were performed for 2D temperature field distribution using ANSYS package. On the basis of the results the conclusion if about the frequency selection as well as the heater location on the railway rail are formulated. They also establish the ground for further three dimensional considerations of the low frequency inductive heating phenomena to specify the heating strategy in practice.

Mathematical modeling

The method of the inductive heating essentially uses eddy current phenomena due to a time varying magnetic field affecting the workpiece (in our case the railway rail). However, one has to take into account that the inductive heating is a complex process involving both electromagnetic and thermal effects. Therefore the electromagnetic-thermal coupling simulation to analyze heat distribution of the rail is needed. The computations were performed for the heating system as illustrated in Fig.1.

In our case both convection current and displacement current densities can be neglected. Therefore, a total current density inside the rail volume is only due to the eddy current J_σ which is related to the electric field intensity $\vec{E}$ by Ohm's law as follows:

$$\vec{J}_\sigma = \sigma\vec{E}\,, \qquad (1)$$

where σ – the rail material electric conductivity.

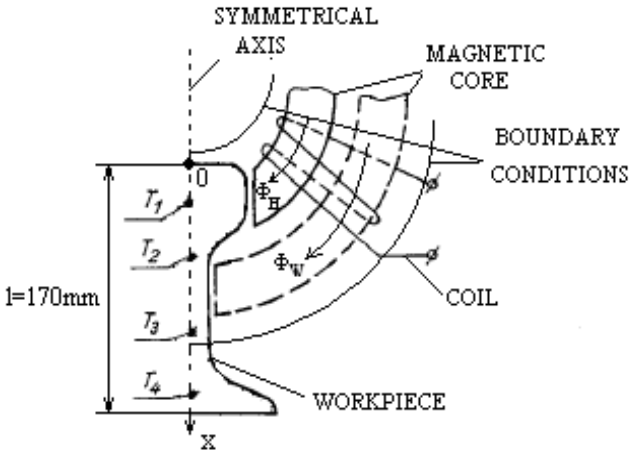

Fig. 1. 1/2 Cross section along the axial symmetry of the inductive heating of the rail for mathematical modeling (Φ_H, Φ_W-flux due to head and web heating respectively, T_1…T_4-points of temperature testing)

Principle of the eddy current field calculation with indicated boundary conditions are shown for clarity in Fig.2.

As a result the Maxwell's equations are expressed in the form:

$$\begin{cases} \nabla \times \vec{H} = \vec{J}_{\sigma}, \\ \nabla \times \vec{E} = -\dfrac{\partial \vec{B}}{\partial t}, \\ \nabla \bullet \vec{B} = 0, \\ \nabla \bullet \vec{J}_{\sigma} = 0, \\ \vec{B} = \mu \vec{H}, \end{cases} \tag{2}$$

where B, H, μ – magnetic flux density, intensity and permeability respectively.

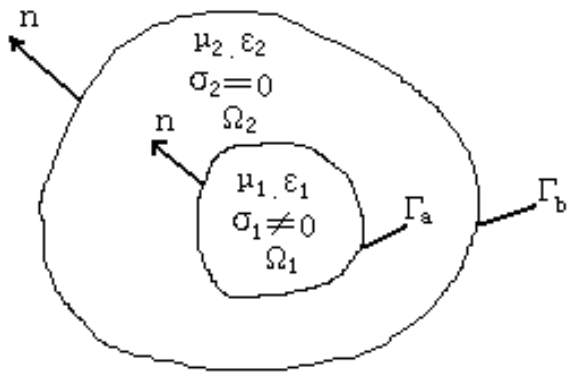

Fig. 2. Illustration of the eddy current field calculations (Γ_a, Γ_b - boundary conditions for eddy current Ω_1 and without eddy current field Ω_2 respectively, μ, ε, σ -permeability, permittivity and conductivity of the analyzed area, n-normal to the surface)

When use vector magnetic potential $\vec{A}$

$$\vec{B} = \nabla \times \vec{A} \tag{3}$$

and substituting it in (2) it gives:

$$\frac{1}{\mu} \nabla \times \nabla \times \vec{A} = \vec{J}_{\sigma} . \tag{4}$$

For the scalar electric potential Φ the above equation (4) can be written in the form

$$\frac{1}{\mu} \nabla \times \nabla \times \vec{A} = -\sigma \frac{\partial A}{\partial t} - \sigma \nabla \Phi , \tag{5}$$

what gives the basic equation for time-varying electromagnetic field. However, this equation can not be solved directly by means of finite element method. To eliminate the scalar electric potential Φ one has to define $\vec{A}'$ and use it instead of $\vec{A}$

$$\vec{A}' = \vec{A} + \int_{-\infty}^{t} \nabla \phi \, dt . \tag{6}$$

Finally equations for $\vec{E}$ and $\vec{B}$ can be expressed as follows:

$$\begin{cases} \vec{E} = -\dfrac{\partial \vec{A}}{\partial t} - \nabla \phi = -\dfrac{\partial \vec{A}'}{\partial t}, \\ \vec{B} = \nabla \times \vec{A} = \nabla \times \vec{A}'. \end{cases} \tag{7}$$

To solve these partial differential equations for the analyzed area it is necessary to specify boundary conditions. Since, in our case magnetic lines are parallel to far-field ($\vec{B}_{1n} = \vec{B}_{2n}$、$\vec{H}_{1t} = \vec{H}_{2t}$、$\vec{J}_{1n} = 0$). Therefore, the modified vector magnetic potential $\vec{A}'$ boundary conditions at the interface are specified as:

$$\begin{cases} \vec{n} \bullet \left(\nabla \times \vec{A}_1{}' \right) = \vec{n} \bullet \left(\nabla \times \vec{A}_2{}' \right), \\ \vec{n} \times \left(\dfrac{1}{\mu_1} \nabla \times \vec{A}_1{}' \right) = \vec{n} \times \left(\dfrac{1}{\mu_2} \nabla \times \vec{A}_2{}' \right), \\ \sigma_1 \left(\dfrac{\partial \vec{A}_1{}'}{\partial t} \right) \bullet \vec{n} = 0. \end{cases} \tag{8}$$

In order to study the thermal effects of the electromagnetic phenomena, one has to combine the above model with the heat equation. Since the analyzed workpieces do not interact thermally, therefore the heating process can be considered separately for the particular workpiece using Fourier's equation:

$$\nabla \bullet \lambda \nabla T - c\gamma \frac{\partial T}{\partial t} = p , \tag{9}$$

where T – temperature; t – time; c – specific heat; γ – mass density; λ – thermal conductivity of the rail material respectively, and p is volume power density.

When neglect power losses due to radiation and include the boundary conditions at the rail surface it is in the form:

$$-\lambda \frac{\partial T}{\partial n} \cong \alpha_c (T_s - T_a) , \tag{10}$$

where subscripts (s,a) denote the surface and ambient temperatures, α_c is heat transfer coefficient and n is the outward normal to the surface.

Flowchart for computations of the combined electromagnetic and thermal process is shown in Fig.3.

Since, in our case the temperature changes with time due to heating are much slower with compare to variation of the electromagnetic field, therefore, one may consider that the electromagnetic time harmonic steady state is obtained for each temperature distribution [2]. The iterations were performed with following 1 to 3 steps:

1. electromagnetic field equation is solved using 2-D

element distributions

2. having obtained the electromagnetic field solution one can compute power density due to eddy-currents what in turn is a source term of the heat distribution equation
3. the heating process equations is solved with 2-D nodal elements using time stepping, what allows for determination of the temperature distribution of the heated workpiece.

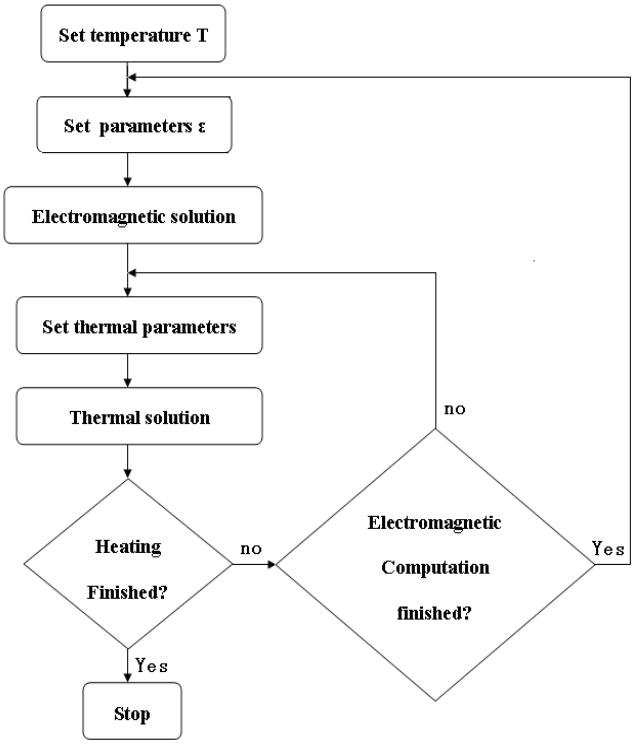

Fig.3. Flowchart of the coupled model

As a matter of fact the all three steps were repeated until the heating process is terminated. Under each iteration the dependence of the thermal parameters were taken into account.

Simulation results and discussion

The computations were carried out using 2D modeling for different frequency of the power source (50 Hz – 900 Hz), different MMF value (500 – 3000 A) and different location of the heater over the railway rail. The temperature distribution along the axis of symmetry at the rail cross section was examined under both heating and consequent cooling process. Particular attention was paid on areas of previously selected points of the rail (T1…T4) at which temperature was able to be measured under experimental investigations. The influence of environment conditions as well as variation of the magnetic properties of the rail material exposed to elevated (over Currie print) temperature was taken under consideration.

Efficiency of heating the rail's head

With point of view of the required heater simplicity its low price and operating comfort the recommended solution seems to be the structure that allows for heating only the rail head. However one has to take into account that the heating process in this case can be highly nonuniform resulting in respective overheating and related excessive thermal stresses within the railway rail body. As a matter of fact the so called neutral temperature value can require delivery of a high energy to rail particularly under heavy duty environmental conditions. Comparison of the heating dynamics for constant power value delivered to the heater (MMF≈2000 A) for two different frequencies can be seen from Fig.4.

It is visible that for relatively short time of heating (equal 100 s) head temperature still keeps its increase (for 450 Hz during about 15 s at point T1) after switching off the power due to the influence of skin effect. The remaining areas (point T2, T3, T4) due to the heat outflow from the head are respectively heated up.

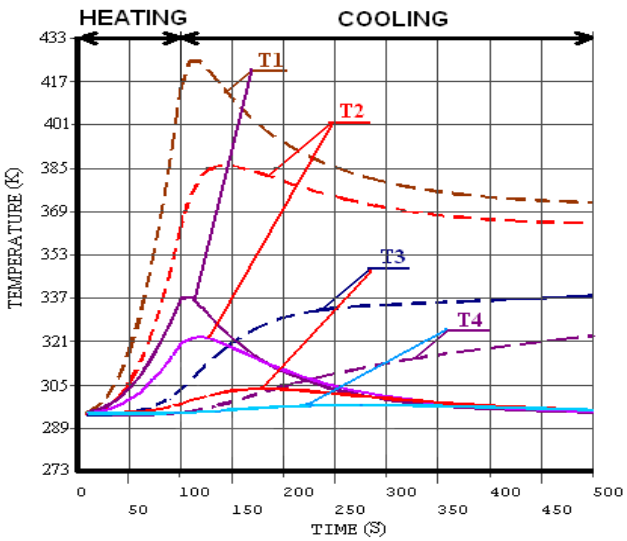

Fig. 4. Temperature distribution in a rail cross section under heating and consequent cooling for 50Hz and 450Hz at MMF≈2000A (heat transfer coefficient=10, ─ 50Hz -- 450Hz)

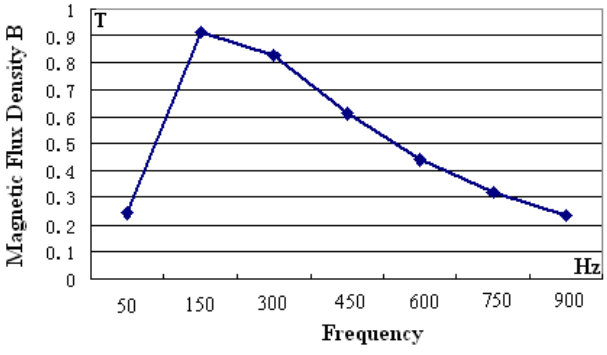

a)

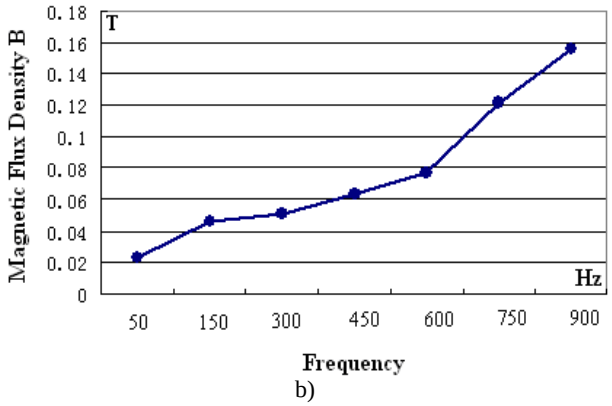

b)

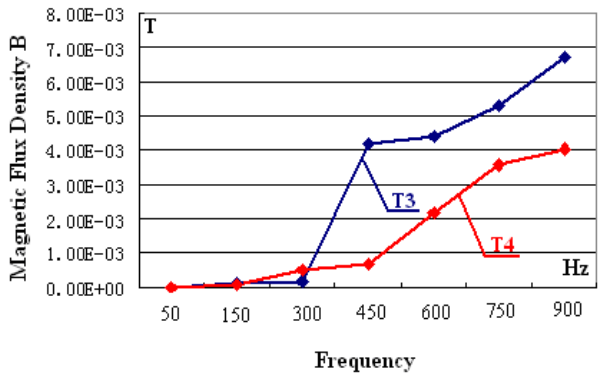

c)

Fig. 5. Variation of magnetic flux density along the rail cross section with frequency at MMF equal 2000A; a) at T_1, b) at T_2, c) at T_3 and T_4

However for the 50 Hz power delivery both field temperature value as well as its dynamics are much less intensive (skin effect is negligible). One has to note that together with the increase of frequency the magnetic field distribution inside the rail is being changed. Magnetic flux density at the head centre reaches its maximum value for 150 Hz and next decreases respectively.

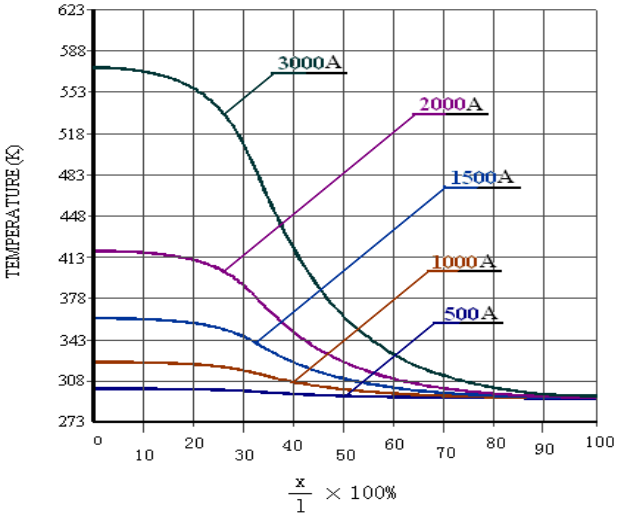

Fig. 6. Influence of MMF value on heating effect at the rail cross section for 450Hz (Heat transfer coefficient=10, heating times 100s)

While the field inside neighbouring areas increases continuously with frequency. It involves also the foot area what is shown in Fig.5. The influence of the MMF value on the heating efficiency is also nonlinear what for 450 Hz is shown for example in Fig.6.

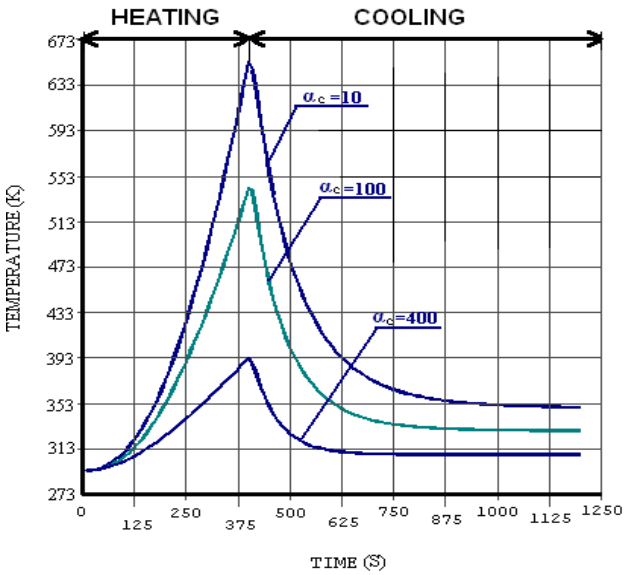

Fig. 7. The influence of environment conditions on heating and cooling effect (Temperature at point T_1) under heating only the head (f=150Hz, MMF≈2000A, α_s=heat transfer coefficient)

Therefore, the heating strategy requires careful consideration of the resulting heating and cooling process, particularly for heavy environment conditions. For example with the increase of the heat transfer coefficient value (α_c) by about 10 times the maximum temperature at T1 decreases by about 20% for 400 s of heating at 150 Hz and 2000 A, what can be seen in Fig.7.

Efficiency of heating both head and web

When heat is produced both at head and web the heating dynamics as well as temperature field distribution are different with compare to these when heating only the head (see Fig. 4 and Fig. 8).

It is related to another field picture (as illustrated in Fig. 9) and another heat source location as a result. The highest temperature value is thus obtained in the web (point T3) what influences the heat outflow from two respective sources. It is worth to note that for the frequency over 100 Hz the magnetic flux over the whole area rail tends to decrease with frequency value.

Comparison of efficiency of heating can be done on the basis of a calculated conventional unit power loss as a function of the frequency (see Fig.10) for two different location of the heat source (heat generated only in head or in head and web simultaneously).

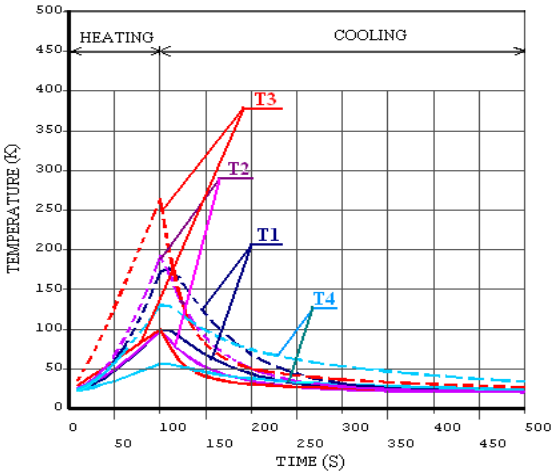

Fig. 8. Temperature distribution in a rail cross section under heating and consequent cooling for 50Hz and 450Hz at MMF≈2000A(Heat transfer coefficient=10, ─ 50Hz, ----450Hz)

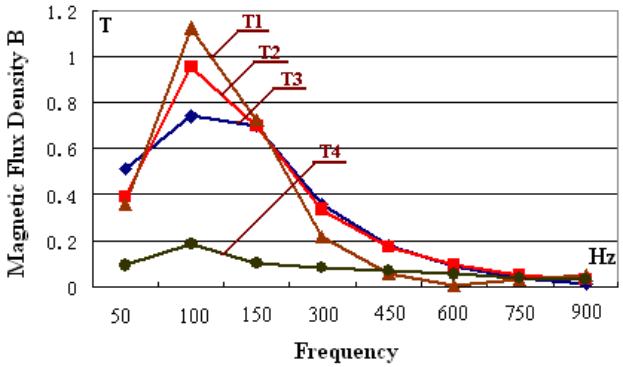

Fig. 9. Variation of magnetic flux density along the rail cross section with frequency at MMF equal 2000A (heater located at head and web)

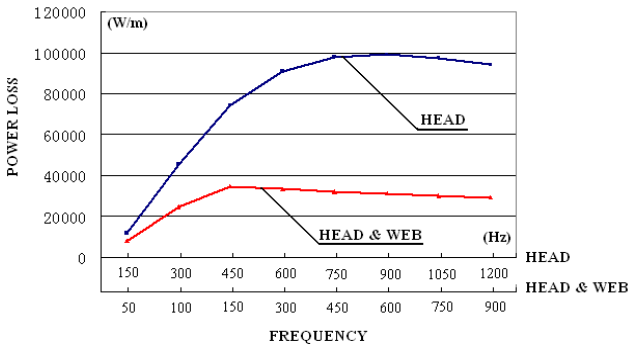

Fig. 10. Comparison of a conventional unit power loss (average over the rail cross section) for different frequency and for two ways of heating (MMF≈2000A)

For the given requirements concerning the heating process one can select both frequency and way of heating as a compromise. For example the same heating effect can be obtained when used the heater located only on the head while increasing frequency to about 150 Hz or for head and web supplied with 50 Hz power source.

Conclusions

The low frequency inductive heating, presented in this paper, that uses the heater system producing the transversal magnetic field, can be satisfactoryly used for heating process of long ferromagnetic elements like railway rails. On the basic of computation results one can conclude that location of the heater both on the head and accessible part of web makes regulation of the heat distribution over the rail cross section possible. It is also possible to consider theoretically the influence of the power source frequency on the magnetic field distribution therefore, on location of the heat source. As a result one can optimize the heating efficiency of the railway rail.

References

1. **Miedzinski B., Okraszewski Z., Szymanski A., Kristiansen M.** Low frequency inductive heating of a rigid track during track lying // Proc. 30th IAS Annual Meeting. Orlando. Florida. USA. – October 8-12, 1995. – P. 1903–1909.
2. **Stoll R. L.** The analysis of eddy currents. – Oxford: Clarendon Press, 1974.
3. **Miedzinski B., Okraszewski Z., Xu L. J., Wang X.** Possibility of Application of a Low Frequency Inductive Heating to Selected Ferromagnetic Objects // Proc. ICREPQ'08. Santander. Spain. – March 11-15. – 2008 (in priting).

Submitted for publication 2008 02 15

B. Miedzinski, Z. Okraszewski, X. Wang, Lj. Xu. Approach to Efficiency of the Low Frequency Inductive Heating of Ferromagnetics // Electronics and Electrical Engineering – Kaunas: Technologija, 2008. – No. 5(85). – P. 3–8.

The heating system using a low frequency supply has been used for heating long ferromagnetic elements. The theoretical considerations using ANSYS program were performed for 2D distributions of the both temperature and magnetic field over the rail cross section. Transversal magnetic field was analyzed for different frequency as well as various MMF of the power source applied. The influence of the heater location and cooling intensity of the environment was taking into account. The calculation results create a basis for further three dimensional considerations allowing for selection of the heating strategy. Ill. 10, bibl. 3 (in English; summaries in English, Russian and Lithuanian).

Б. Мэдзински, З. Окрашевски, Х. Ванг, Ли. Ху. Анализ эффективности ферромагнитного нагревателя переменного тока низкой частоты // Электроника и электротехника. – Каунас: Технология, 2008. – № 5(85). – С. 3–8.

Описывается распределение магнитного поля в двухмерном пространстве, когда для теоретического анализа применена ANSYS программа. Магнитное поле рассматривается для разных частот поля и источников питания. Предлагаются основы расчета и для трехмерного пространства. Полученные результаты позволяют выбрать оптимальную стратегию отопления. Ил. 10, библ. 3 (на английском языке; рефераты на литовском, английском и русском яз.).

B. Miedzinski, Z. Okraszewski, X. Wang, Lj. Xu. Feromagnetikų kaitinimo žemojo dažnio indukciniu kaitintuvu efektyvumo analizė // Elektronika ir elektrotechnika. – Kaunas: Technologija, 2008. –Nr. 5(85).– P. 3–8.

Ilgiems feromagnetiniams elementams kaitinti buvo panaudota kaitinimo sistema su žemojo dažnio maitinimo šaltiniu. Temperatūros ir magnetinio lauko pasiskirstymas dvimatėje erdvėje buvo ištirtas teoriškai, naudojant ANSYS programą. Skersinis magnetinis laukas analizuotas esant skirtingiems lauko dažniams bei skirtingiems maitinimo šaltinio MMF. Atsižvelgta į kaitintuvo buvimo vietą ir aplinkos aušinimo intensyvumą. Remiantis skaičiavimo rezultatais ateityje bus galima atlikti analogiškus tyrimus trimatėje erdvėje. Tyrimo rezultatai naudingi optimaliai šildymo strategijai parinkti. Il. 10, bibl. 3 (anglų kalba; santraukos anglų, rusų ir lietuvių k.).